Numerical investigation on the thermo-mechanical behavior of HTS tapes and experimental testing on their critical current

D. P. Boso, *Fellow, IEEE,* M. Breschi, *Senior Member, IEEE,* A. Musso, E. Pilastro, P. L. Ribani, *Fellow, IEEE*

***Abstract*—This work extends to second generation Rare-Earth Barium-Copper-Oxide ((Re)BCO) tapes an experimental procedure previously developed to analyze the impact of double bending at room temperature on the performance of Bismuth-Strontium-Calcium-Copper-Oxide (BSCCO) tapes. The modified procedure is applied to measure the critical current of a commercial (Re)BCO tape subjected to bending around a cylindrical mandrel first on one side, then on the other side, followed by the cooldown to cryogenic temperature. In the bending phase, mandrels of decreasing diameter are used to identify the minimum curvature leading to a significant reduction of the tape critical current. Furthermore, a novel finite element model is developed to complement the experimental results. The model simulates the double bending at room temperature, the following straightening of the sample, and its cooldown to cryogenic conditions. The coupled thermo-mechanical numerical model together with the temperature-dependent mechanical properties allow investigating the combination of thermal contraction effects and bending loads in the whole domain of the problem. The experimental and numerical results obtained help to give a better insight in the distribution of the strain and stress components inside the (Re)BCO tape and to evaluate their impact on the conductor electrical performance in relevant operating conditions.**

***Index Terms*—HTS tapes, Finite element methods, Strain distribution, Critical current measurement**

I. Introduction

The High Temperature Superconducting (HTS) materials are considered as possible candidates for application to high field magnets, e.g. for fusion and high-energy physics, and to AC or DC power applications. The development of HTS conductors requires extensive information about the impact of the cable architecture on the electrical performance of the superconducting tapes or wires. In particular, for a proper conductor design, it is important to characterize the bending behavior of the tape. Recently, a significant effort to investigate in this direction was performed both with experimental and numerical studies [1]-[7].

In this work, a measurement procedure is applied to determine the critical current of the tape when subjected to a bending deformation on its two opposite sides (the so called "double bending", see e.g. [8]) at room temperature, followed by the cooldown to cryogenic conditions. In the flexural phase, mandrels of decreasing diameter are used.

Additionally, a novel finite element model is developed to analyze the experimental results. As a first step, the double bending is simulated, followed by the straightening of the sample as a second step. Finally, in the third step the cooldown to 77 K is modelled, thus computing the final strain field.

II. The Experimental Procedure

The procedure for the measurement of critical current of Rare-Earth Barium-Copper-Oxide ((Re)BCO) tapes after double bending at room temperature is derived by extending with some modifications a similar procedure developed for Bismuth-Strontium-Calcium-Copper-Oxide (BSCCO) tapes [8], which led to the publication of an IEC standard [9].

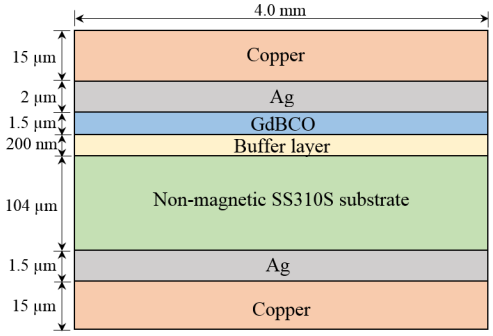

Fig. 1. Geometry of the cross-section of the SuNAM SCN04 model tape (not to scale).

The specimen used in the present work is a SCN04 model tape manufactured by SuNAM Co., Ltd. The superconducting layer is composed of $GdBa_2Cu_3O_7$ (GdBCO). Fig. 1 presents its cross-section and the dimensions of each layer. The tape samples are 30 cm long.

The procedure is carried out as follows. First of all, the tape is cooled down in liquid nitrogen and its critical current is measured to determine its reference value before the application of external mechanical loads. The specimen is mounted on a rigid G10 straight support having the same length of the tape, and both ends of the tape are pressed onto the holder using two 10

Manuscript received and acceptance dates will be inserted here.

D. P. Boso and E. Pilastro are with the Department of Civil, Environmental and Architectural Engineering of the University of Padova, Padova, 35131, Italy (e-mail: daniela.boso@unipd.it, eugenio.pilastro@studenti.unipd.it).

M. Breschi, A. Musso, and P. L. Ribani are with the Laboratory of Magnet Technology and Applied Superconductivity of the University of Bologna, Bologna, 40136, Italy (e-mail: marco.breschi@unibo.it, andrea.musso3@unibo.it).

cm long copper bars. This length has been set to allow the current to distribute from the current lead to the tape without causing excessive heating due to the contact resistance. Indium is not used between the tape and the copper bar. Pressure is maintained using brass screws, without solder. The voltage taps are placed in the central part of the tape, clipped onto its surface, at a distance of 5 cm to each other, without solder. Not soldering is very important to avoid any additional mechanical stress during the bending process. An image of the specimen on the holder is shown in Fig. 2(a); note that the distances between the various taps are consistent with the criteria described in [9].

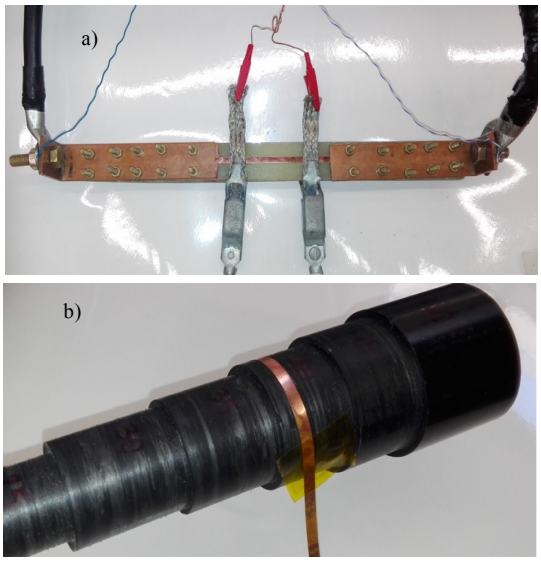

Fig. 2. (a) HTS tape laid over the straight sample holder and connected to current leads. (b) HTS tape bent over the mandrel.

The sample is immersed in liquid nitrogen and the measurement is carried out in self-field. After the measurement, the specimen is warmed up to room temperature and the double bending procedure is carried out. As a first step, one section of the tape is fixed on a mandrel with a certain diameter. The fixed point is close to the region of the tape that was not immediately covered by the copper bars during the straight test. One of the two free regions of the tape, the portion including voltage taps, is gradually bent along the mandrel from the fixed point to the next tape section previously covered by the second copper bar, as shown in Fig. 2(b). In this way, the whole region between the voltage taps is certainly bent. The sample is then released and free from constraints. The same procedure is repeated by turning the tape on its opposite face and bending exactly the same tape portion. Finally, the tape is straightened again, repositioned on the sample holder, cooled down in nitrogen, and subjected again to the critical current measurement. It should be noted that some layers of the tape, in particular the copper layer, may have plasticized during the bending procedure, and the tape may consequently result bent even when left free. In order to lay the tape over the rectilinear support, one end is first fixed below one of the two copper bars and the free end is slowly straightened to get it below the second copper bar.

After the critical current measurement, the tape is removed and a new sample is placed on the holder, repeating the procedure with a mandrel of different diameter.

III. The Numerical Model

The numerical model developed is based on a coupled thermo-mechanical approach, with temperature dependent material characteristics. Given the high aspect ratio of the tape sample – with a length of 300 mm and a thickness of 0.139 mm – and the thinness of the (Re)BCO layer, an effective finite element discretization operated by means of 3D continuum elements would require millions of elements, thus resulting in millions of degrees of freedom. To avoid this, homogenization procedures could be used [10]-[13]. On the other side, HTS tapes can be considered thin-walled structures where in-plane components of the strain and stress fields play a major role. Shell elements are suitable to model this type of geometric domains, in which one dimension (the thickness) is significantly smaller than the other two. In this way, the formulation of the problem is restricted to a 2D domain, and only the reference surface needs to be discretized. Concerning the presence of several materials, in this study multi-layered composite shell elements are used. In detail, shell elements with 4 nodes and 6 degrees of freedom per node are chosen, with reduced integration (1 Gauss point in the mean plane) to avoid spurious modes and to optimize the computational cost. In the out of plane direction, to reconstruct in detail the stress and strain distributions across the tape thickness, the composite layup-type section is made of 6 layers, and 3 Simpson integration points per layer are used. The whole 4x300 mm sample was modelled, for a total of 5587 elements, 9807 nodes and 19056 degrees of freedom.

All analyses were run considering large displacement, finite strain formulation, elastic-plastic materials for copper, substrate and silver, linear elastic behavior for (Re)BCO. Finally, contact phenomena with the surface of the mandrel were also implemented. The commercial software ABAQUS® [14] was used for the computations.

Concerning the material characteristics, unfortunately it is very difficult to find a consistent set of data for the temperature range of interest. In the following, for the cryogenic temperature, we consider mainly the material characteristics found in [15]. With these mechanical parameters at hand, the tape behavior at 77 K was validated against the stress-strain curve available from SuNAM [16]. Concerning the room temperature characteristics, ad hoc experimental tests were performed to measure the global behavior of the tape, as described in the following section.

A. Measurement and simulation of the stress-strain curve of the (Re)BCO tape at room temperature

The measurements of the stress-strain curve under a tensile load were performed at the University of Padova, by applying the following procedure. Each sample was mounted on a Galdabini SUN/2500 machine (25 kN maximum force, based on the UNI EN ISO 7500-1 standard, accuracy class 0.5). The tests were conducted by applying controlled displacements at the sample ends at a very low velocity (5 mm/min), in order to avoid inertial effects. The sampling frequency of loads and displacements was 15 ms. The nominal strain was calculated by dividing the applied displacement by the initial sample length, the corresponding stress was obtained by dividing the recorded force by the cross section of the tape.

In the related finite element computations, a straight tape was considered as a starting configuration; the longitudinal degrees of freedom were constrained at the first raw of nodes at one end, while displacements were applied to the nodes at the other end.

Fig. 3 reports the comparison of the stress - strain curve obtained numerically with the results of the experiments at 77 K and 293 K. The simulation results for both temperatures exhibit a good agreement with the experimental stress–strain curves. The material data validated by this comparison were then used for the simulation of the double bending experiments; the main parameters are reported in Table I. The material characteristics over the temperature range of interest were reconstructed by linear interpolation.

TABLE I
MATERIAL DATA USED IN THE FINITE ELEMENT MODEL

Temperature [K]	Material	Young modulus [GPa]	Yielding limit [MPa]	Plastic modulus [GPA]	Thermal contraction coefficient [1/K]
77	Substrate	179.5	725	10	1.34E-05
77	Copper	85	350	4	1.77E-05
77	Silver	90	225	22	1.90E-05
77	(Re)BCO	140	-	-	1.00E-05
293	Substrate	125	350	4.9	1.34E-05
293	Copper	85	350	4	1.77E-05
293	Silver	90	225	22	1.9E-05
293	(Re)BCO	150	-	-	1.00E-05

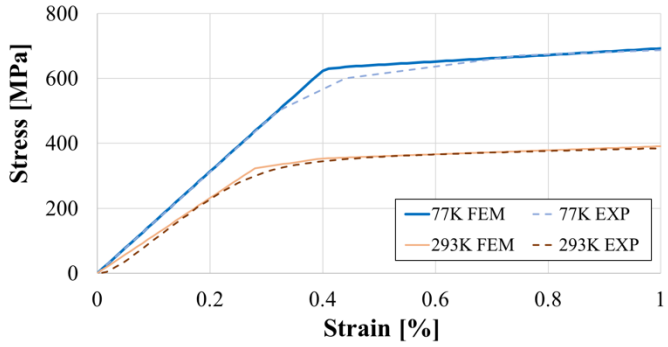

Fig. 3. Longitudinal behaviour of the tape: comparison between experimental (dashed lines) and numerical results (continuous lines). The experimental data shown are obtained by averaging over five sample results.

B. *Simulation of the double bending experiments*

The finite element analyses performed consist of three steps. In the first one the double bending is modelled, by considering the mandrel as a rigid surface and applying a uniform pressure on one side of the tape, then releasing the load and applying it to the other side. Concerning the boundary conditions, the longitudinal degrees of freedom were constrained at the first raw of nodes at one end, while all the other nodes were left free. In the second step, the pressure was removed and suitable displacements were applied to the unconstrained tape end, to recover the initial straight configuration. Finally, in the third step, the cooldown from 293 K to 77 K was modelled, by applying a uniform decrease of temperature to all the nodes of the mesh, divided into ten equal steps. The simulations were repeated for 4 different mandrel diameters, namely 10, 12.5, 15 and 20 mm.

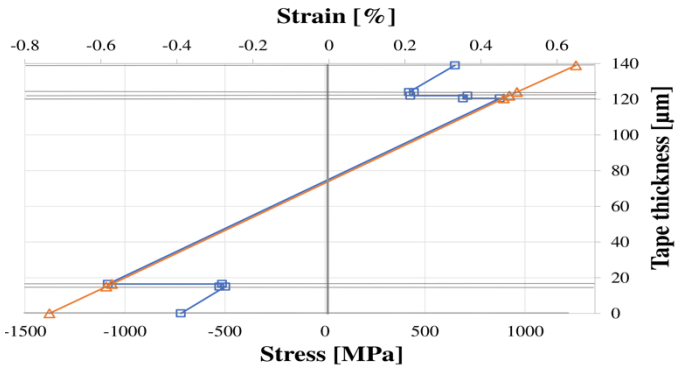

Fig. 4. Stress (on the bottom axis) and strain (on the top axis) distribution along the tape thickness.

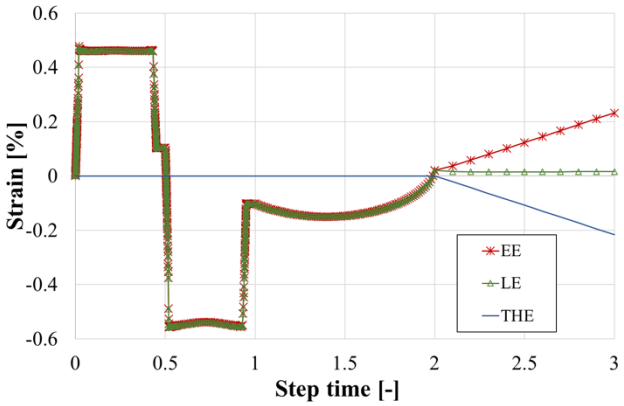

Fig. 5. Evolution of the strain components in the (Re)BCO layer during the double bending at room temperature around a mandrel with a 20 mm diameter (0-1), tape straightening (1-2) and final cooldown (2-3). Green line: total logarithmic strain (LE), blue line: thermal strain (THE), red line: elastic strain (EE).

The finite element model developed allows computing the strain and stress fields in the whole domain of interest. Fig. 4 shows the distribution of the longitudinal strain and stress components in the various tape layers. Since there is no delamination, the strain is linear across the thickness (orange line with triangles), while the jumps in the stress values (blue line with squares) are due to the different Young moduli of the materials involved.

For the 20 mm diameter taken as exemplifying case, the evolution of the thermal, elastic and total longitudinal strain in the barycenter of the (Re)BCO layer is shown in Fig. 5. The measure of strain is logarithmic as properly computed for large deformation regimes. The total strain (LE) is given by the sum of the elastic (EE) and thermal (THE) contributions. It can be noted that in the (Re)BCO layer the maximum strain is reached during the double bending phase, with a slight difference between the absolute values reached in tension and compression, due to the asymmetric position of the superconducting material with respect to the neutral axis.

During the bending phase, the silver and copper layers reach their yielding limit. For example, the longitudinal strain occurring in the top copper layer is plotted in Fig. 6. It is clearly visible that the plastic strain contribution (PE) develops shortly after the beginning of the first bending, it becomes compressive

during the second bending and then remains constant till the end of the cooldown.

Finally, Fig. 7 summarizes the strain values in the (Re)BCO layer obtained for the 4 different diameters mentioned above.

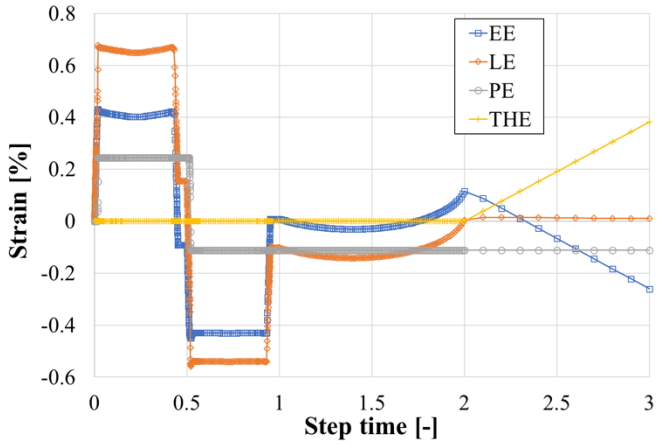

Fig. 6. Evolution of the strain components in the top copper layer during the double bending at room temperature around a mandrel with a 20 mm diameter (0-1), tape straightening (1-2) and final cooldown (2-3), with the grey line representing the plastic contribution (PE).

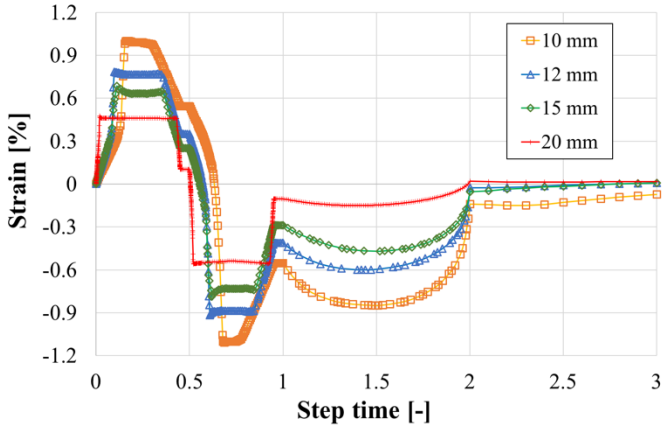

Fig. 7. Evolution of the total longitudinal strain in the (Re)BCO layer for different mandrel diameters.

IV. Experimental Results and Discussion

As anticipated in Section II, the double bending experiments were repeated adopting mandrels of different diameter, starting from 50 mm and progressively reducing it to 12 mm. The tolerance in the diameter value is ± 0.5 mm for all the mandrels prepared for this work. For each of the studied diameters, the whole procedure was repeated twice, by changing the tape sample. A good reproducibility of the results was recorded, thus giving confidence in the experimental procedure adopted. Fig. 8 shows the critical current values obtained in the tests. It can be noticed that the tape shows a clear threshold behavior between the diameters of 15 mm, for which the tape is not degraded, and 12.5 mm, when a dramatic reduction of the critical current is found.

The results of the numerical model presented in section III help interpreting the obtained experimental results. Given a mandrel diameter, the FE analysis calculates the strain field during the whole experiment. The longitudinal strain reaches its peak value during the double bending phase and decreases in the following steps. This behavior suggests that the abrupt degradation of the (Re)BCO layer for mandrel diameters below 15 mm occurs during the double bending at room temperature. Furthermore, since the final strain field at 77 K is significantly lower than the peak values reached during the bending procedure, the investigation of the complete mechanical history of the tape seems mandatory.

The numerical model allows identifying the threshold strain level which must not be overcome to avoid the dramatic drop of the tape performances. In particular, between the 15 mm and 12.5 mm diameter cases the numerical model calculates a strain value in the (Re)BCO layer ranging from 0.75 to 0.9%, which exceed the irreversible strain limit of the tape [16].

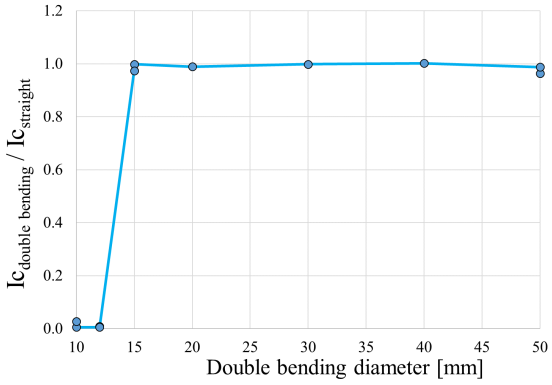

Fig. 8. Experimental results of the double bending procedure with different diameter

V. Conclusion

A set of measurements of critical current of (Re)BCO tapes subjected to double bending at room temperature was performed by extending an experimental procedure previously developed for BSCCO tapes. The results of the test campaign clearly indicated, for the investigated SuNAM tape, the existence of a threshold mandrel diameter (included between 12.5- and 15- mm) below which the critical current of the tapes dramatically drops. A novel finite element model was developed to compute the strain distribution in the tape under bending and thermal loading. The model showed that the strain in the (Re)BCO layer reaches its maximum during the double bending phase, with values in the range from 0.75 to 0.9%, which exceed the irreversible limit of the tape. The abrupt performance drop found in the experiments suggests a possible rupture of the (Re)BCO layer.

Acknowledgment

The authors would like to thank Hanwoo Cho from SuNAM Co., Ltd. for providing the stress-strain characteristics at 77 K and Marco Vittadello from the University of Padova for performing the stress-strain measurements at room temperature.

REFERENCES

[1] A. Gorospe, Z. Bautista, H. S. Shin, H. Oguro, and S. Awaji, "Characteristic irreversible critical strain limit of GdBCO-coated conductor tapes under various temperature and magnetic field conditions," *IEEE Trans. Appl. Supercond.*, vol. 27, no. 4, Jun. 2017, Art. no. 8400205.

[2] P. Sunwong, J. S. Higgins, and D.P. Hamsphire, "Probes for investigating the effect of magnetic field, field orientation, temperature and strain on the critical current density of anisotropic high-temperature superconducting tapes in split-pair 15 T horizontal magnet," *Rev. Scientific Instrum.*, vol. 85, 2014, Art. no. 065111.

[3] M. A. Diaz and H. S. Shin, "Variations of the Strain Effect on Critical Current in REBCO Coated Conductor Tapes Depending on Test Probes," *IEEE Trans. Appl. Supercond.*, Vol. 29, no. 5, Aug. 2019, Art. no. 8400905.

[4] M. Breschi, E. Berrospe-Juarez, P. Dolgosheev, A. Gonzalez-Parada, P. L. Ribani, F. Trillaud, "Impact of Twisting on Critical Current and n-value of BSCCO and (Re)BCO Tapes for DC Power Cables," *IEEE Trans. Appl. Supercond.*, vol. 27, no. 4, 2017, Art. no. 5401404.

[5] K. Ilin, K. A. Yagotintsev, C. Zhou, P. Gao, J. Kosse, S. J. Otten, W. A. J. Wessel, T. J. Haugan, D. C. van der Laan, and A. Nijhuis, "Experiments and FE modeling of stress–strain state in ReBCO tape under tensile, torsional and transverse load," *Supercond. Sci. Technol.,* Vol. 28, 2015, Art. no. 055006.

[6] M. Takayasu and L. Chiesa, "Analytical investigation in bending characteristic of twisted stacked-tape cable conductor," *IOP Conf. Series: Materials Science and Engineering*, Vol. 102, 2015, Art. no. 012023.

[7] L. Chiesa, M. Takayasu, N. C. Allen, and L. Bromberg, "Electromechanical Investigation of Different Type YBCO Tapes for Twisted Stacked-Tape Cabling," *IEEE Trans. Appl. Supercond*, vol. 23, no. 3, 2013, Art. no. 4800205.

[8] Y. Yamada *et al.*, "International round robin test of the retained critical current after double bending at room temperature of Ag-sheathed Bi-2223 superconducting wires," *Supercond. Sci. Technol.*, vol. 29, no. 2, Feb. 2016, Art. no. 025010.

[9] IEC 61788-24. *Critical Current Measurement—DC Critical Current of Ag- and/or Ag Alloy-Sheathed Bi-2212 and Bi-2223 Oxide Superconductors*, 2nd edn, 2018.

[10] M. Lyly, *et al.*, "Validation of homogenized filament bundle model in AC loss computations," *IEEE Trans. Appl. Supercond.*, vol. 2, no. 3, Jun. 2012, Art. no. 4705505.

[11] M. Lefik *et al.*, "Generalized self-consistent homogenization using the finite element method," *ZAMM · Z. Angew. Math. Mech.* 89, No. 4, 306 – 319 (2009), DOI 10.1002/zamm.200800215

[12] A.A. Amin, "Computational homogenization of the elastic and thermal properties of superconducting composite MgB2 wire," *Composite Structures,* Vol. 188, Mar. 2018, 313-329

[13] D. Boso *et al*., "Macroscopic damage in periodic composite materials," *Commun. Numer. Meth. Engng* 2000; 16:615–623, DOI: 10.1002/1099-0887(200009)16:9<615::AID-CNM355>3.0.CO;2-2

[14] Abaqus Unified FEA - SIMULIA by Dassault Systemes //www.3ds.com/products-services/simulia/products/abaqus

[15] N. C. Allen, L. Chiesa, and M. Takayasu "Structural modeling of HTS Tapes and Cables," *Cryogenics*, Vol. 80, 405-418, 2016.

[16] SuNAM Co., Ltd., private communication.